Modeling confinement in Étang de Thau: numerical simulations and multi-scale aspects

Jean-Philippe Bernard[*], Emmanuel Frénod[†] and Antoine Rousseau[‡]

2012, August 30th

1 Introduction

The main purpose of this paper is to implement a mathematical model of confinement in a realistic configuration; the model we consider here relies on a previous work by two of the authors in [FR12]. The concept of confinement was introduced by Guelorget and Perthuisot [GP83a] in 1983. It has latter been widely used, studied, discussed and tested (see Guélorget and Perthuisot [GP83b, GP83a], Guélorget, Frisoni and Perthuisot [GFP83], Guélorget *et al.* [GGLP90], Ibrahim *et al.* [IGF+85], Debenay, Perthuisot and Colleuil [DPC93], Redois and Debenay [RD96], Barnes [Bar94], Frénod and Goubert [FG07] and Tagliapietra *et al.* [TSG09]) leading to the conclusion that it is a pertinent parameter controlling the features of living benthic population in paralic ecosystems. Benthic species are species living on the seabed and paralic ecosystems are ecosystems encountered in estuaries, lagoons and closed bays. This is a first motivation to conduct numerical simulations of confinement in a lagoon.
In addition, since the confinement of an area is closely related to the amount of available nutrient, we will implement our model in a lagoon where shellfishes are farmed, here *Étang de Thau*, located on the French Mediterranean shoreline.

We start with recalling in Section 2 the mathematical model introduced in [FR12]. Then, we perform in Section 3 the numerical simulations of confinement in *Étang de Thau*, and discuss how to get rid of the spurious oscillations that occur because of the lack of smoothness of the computational domain. Finally, we introduce in Section 4 a method that allows to account for multi-scale aspects of embedded lagoons. This method is based on the theory of *absorbing boundary conditions* first introduced in [EM77], and is implemented here in a very simple case.

2 Mathematical modeling

In this section, we want to introduce the mathematical model that will be used in the sequel to compute confinement fields in *Étang de Thau*. This model is similar to the PDE model introduced by two of the autors and we refer the interested reader to [FR12] for additional details.

[*]Inria, Moise & Université de Reims Champagne-Ardenne
[†]LMBA (UMR 6205), Université de Bretagne-Sud & Inria Nancy Grand-Est
[‡]Moise, Inria Grenoble Rhône-Alpes / Laboratoire Jean Kuntzmann (UMR 5224)

2.1 Definitions

The first mathematical definition of confinement was provided by Frénod and Goubert (see [FG07]) as a controlling parameter of tide-influenced paralic ecosystems:

Definition 1 *The **confinement** value at any point of the lagoon is the time for the sea-water to reach this point.*

In order to account for possible time-oscillations (*i.e.* tidal oscillations), Frénod and Rousseau extended the definition in [FR12]:

Definition 2 *The **instantaneous confinement** is, at a given point of the lagoon and at a given time, the amount of time the water which is at the considered time at the considered point has spent inside the lagoon water mass.*

Definition 3 *The **effective confinement** is the time-average of the instantaneous confinement over its oscillating period.*

2.2 Transport equation for confinement

We consider (see Figure 1) that the lagoon is a cylinder with base a regular, connected and bounded domain $\Omega \subset \mathbb{R}^2$ with boundary $\partial\Omega$. This boundary is shared into $\overline{\Gamma}$ and Γ_0 with $\overline{\Gamma} \cap \Gamma_0 = \emptyset$. Any point in $\overline{\Omega}$ is denoted (x, y). The lagoon seabed is described by a piecewise continuous function $b : \Omega \longrightarrow \mathbb{R}^+$, where $b(x, y)$ represents the bathymetry level at the horizontal position $(x, y) \in \Omega$. The water altitude h is such that $h > \sup_\Omega\{b\}$, exluding outcrops. In summary, the geometrical model of the lagoon writes:

$$\Big\{(x, y, z),\ (x, y) \in \Omega,\ b(x, y) < z < h\Big\}. \tag{1}$$

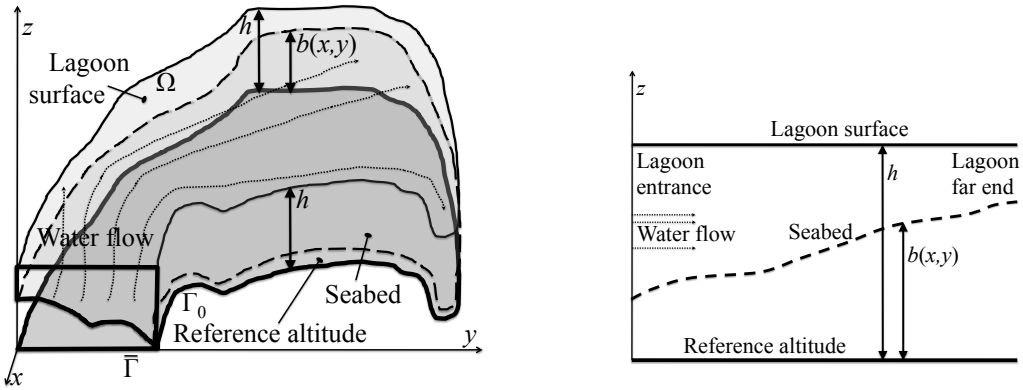

Figure 1: Left: Lagoon geometry; Right: A section of the Lagoon geometry over a line going from the Lagoon entrance to the Lagoon far end.

In order to compute the instantaneous confinement, we use a passive tracer g_t (see below) advected by the water velocity field $\boldsymbol{u}$. As shown in [FR12], this model is compatible with any lagoon geometry (shape and bathymetry), with the only restriction that intertidal zones and seabed outcrops are not taken into account. The idea developped in [FR12] is to solve the following transport problem: for any time $t > 0$ and given a sufficiently large time T, the solution

$g_t = g_t(\tau, x, y)$ of

$$\left\{ \begin{array}{rcll} \dfrac{\partial g_t}{\partial \tau}(\tau,x,y) + \boldsymbol{u}(t-T+\tau,x,y)\cdot\nabla g_t(\tau,x,y) & = & 0, & \forall 0<\tau<T, \forall (x,y)\in\Omega, \\ g_t(\tau,x,y) & = & T-\tau, & \forall 0<\tau<T, \forall (x,y)\in\overline{\Gamma}, \\ g_t(0,x,y) & = & T, & \forall (x,y)\in\Omega, \end{array} \right. \tag{2}$$

is such that $g_t(T, x, y)$ is the value of the instantaneous confinement at time $t \in \mathbb{R}_+$ and position $(x, y) \in \Omega$, where the water velocity field $\boldsymbol{u}(t, x, y)$ may be computed by solving the following equation:

$$\left\{ \begin{array}{rcll} -\nabla\cdot\big[(h-b)\boldsymbol{u}\big](t,x,y) & = & \theta(t,x,y), & \forall t\in\mathbb{R}, \forall (x,y)\in\Omega, \\ \boldsymbol{u}\cdot n & = & F(t,x,y), & \forall t\in\mathbb{R}, \forall (x,y)\in\overline{\Gamma}, \\ \boldsymbol{u}\cdot n & = & 0, & \forall t\in\mathbb{R}, \forall (x,y)\in\Gamma_0, \end{array} \right. \tag{3}$$

where F is a function defined on $\overline{\Gamma}$ such that :

$$\int_{\overline{\Gamma}} \big[(h-b)F\big](t,x,y)\,\mathrm{d}l = \int_\Omega \theta(t,x,y)\,\mathrm{d}x\,\mathrm{d}y,\ \forall t\in\mathbb{R}. \tag{4}$$

The velocity field $\boldsymbol{u}$ can be separated in several "elementary" velocity fields, each of those being solely induced by one single process (such as evaporation, tide, river input, etc.). Consequently, depending on those processes, the function θ can model several phenomena.

Remark 1 *If we consider a tide-submitted lagoon, the domain Ω is time-depending. The reader can refer to [FR12] for more details.*

3 Numerical simulations in a realistic geometry

In order to extend the results of [FR12], we now proceed to a numerical simulation of confinement in a realistic geometry. We consider the case of a lagoon on the French Mediterranean shoreline: *Étang de Thau* (see Figure 2).

3.1 Étang de Thau

Étang de Thau is one of the largest lagoons on the French Mediterranean coastline. It is more than 20km long, from Balaruc-les-Bains (NE end) to Marseillan (SW). A lot of shellfishes live in this lagoon: Thau is famous for its oyster and mussel farms (see [DDG75]). This lagoon is constantly monitored because it is a very sensitive area with regard to eutrophication [AAB+99]. The sale of oysters and mussels has even been prohibited several times since the late 80's. Indeed, eutrophication induces an ecosystem deficiency: high densities of nitrogen and phosphor make macroalgae and phytoplankton proliferate, which disturbs herbarium development. Finally, this leads to spats infirmity in the shellfish farms and ends with weak crops.
In order to quantize eutrophization of a lagoon, we first consider its confinement, with the natural idea that the more an area is confined, the more it is subject to eutrophication.

In *Étang de Thau*, most of the seawater flux comes from the Mediterranean Sea by the *Graus de Pisse-Saumes* (0.75×10^6 m^3 by day) and Sète's channels (3.7×10^6 m^3 by day). Fresh water comes from the rain (48×10^6 m^3 by year) and river input (30×10^6 m^3 by year) [A.62]. In our numerical simulations, we will account for both seawater sources, in the (simple) case where the evaporation rate $\theta > 0$ is constant, letting time and space variations of θ to subsequent studies. Thanks to data provided by the Languedoc-Roussillon Region, we have built two meshes of the lagoon including its bathymetry map (see Figure 2) on which we will perform numerical simulations of the model introduced in Section 2.

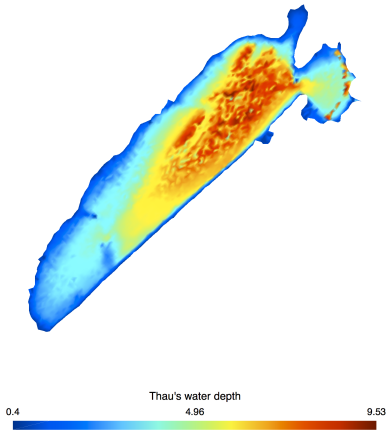

Figure 2: Étang de Thau: bathymetry map provided by Languedoc-Roussilon region

3.2 Viscosity and mesh influences

In order to compute confinement in *Étang de Thau*, we plugged the mesh and bathymetry informations into the software implemented by Frénod and Rousseau in [FR12], thanks to the finite element toolbox *FreeFem++* [HPLH04].
Because of non regular boundaries, the corresponding numerical solutions include spurious numerical oscillations. To overcome this problem, we could either add some artificial viscosity in the model, or try to use a finer mesh. In the case where a viscous model is used, we have:

$$\left\{\begin{array}{rcll} \dfrac{\partial g_t}{\partial \tau}(\tau,x,y)+\boldsymbol{u}(t-T+\tau,x,y)\cdot\nabla g_t(\tau,x,y)+... & & & \\ ...-\nu\Delta g_t(\tau,x,y) & = & 0 & \forall 0<\tau<T, \forall (x,y)\in\Omega, \\ g_t(\tau,x,y) & = & T-\tau & \forall 0<\tau<T, \forall (x,y)\in\overline{\Gamma}, \\ g_t(0,x,y) & = & T & \forall (x,y)\in\Omega, \end{array}\right. \tag{5}$$

where ν is the (dimensionnal) artificial viscosity.
Figures 3c and 3d correspond to the same coarse grid and the simulation is run with the same parameters in Equation (5), except the viscosity that is changed from 100 to 400.[1] The reader can see the oscillations occuring in Figures 3a and 3b (white parts of the plot), close to the two entrances; these oscillations disappear with an increased viscosity (Figures 3e and 3f), but the solution has artificially spread inside the domain (Figures 3c and 3d).

Alternatively, we tried to avoid the numerical oscillations whilst keeping a small viscosity: this necessitates a finer mesh, and was done in Figure 4d. The numerical simulation is improved with respect to Figure 3c, without any artificial spread (as in Figure 3d). Naturally, this last simulation is computationally more demanding, since the time step has to be reduced together with the mesh size (for obvious stability reasons).

[1] One may first think that these viscosity values are way too high (unphysical), but we want to point out that those values correspond to orders of magnitude of 10^{-6} in a nondimensionnal system (remember that the lagoon is $2.10^4 m$ long). Consequently, the additional term has very little influence on the tracer g_t that remains mainly driven by the velocity. The viscosity (at least for reasonably small values) only smoothes the solution.

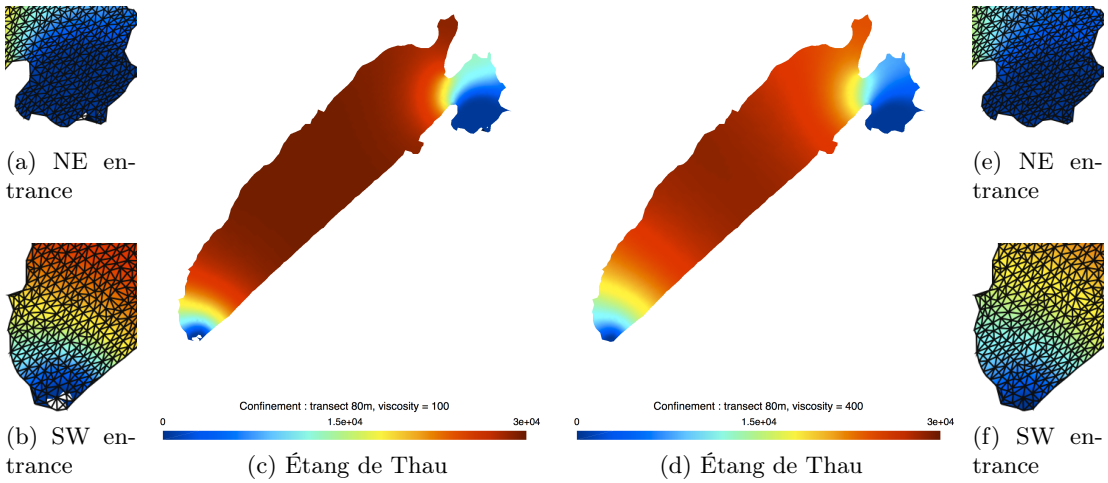

(a) NE entrance (b) SW entrance (c) Étang de Thau (d) Étang de Thau (e) NE entrance (f) SW entrance

Figure 3: Confinement field in *Étang de Thau* with zooms in the NE and SW entrances. Left: $\nu = 100$, $meshsize = 80m$. Right: $\nu = 400$, $meshsize = 80m$.

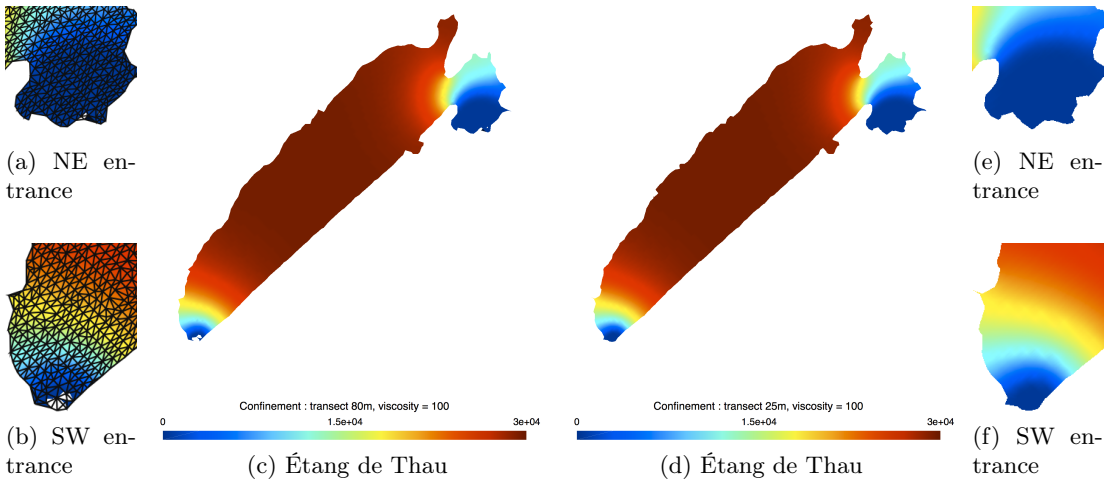

(a) NE entrance (b) SW entrance (c) Étang de Thau (d) Étang de Thau (e) NE entrance (f) SW entrance

Figure 4: Confinement field in *Étang de Thau* with zooms in the NE and SW entrances. Left: $\nu = 100$, $meshsize = 80m$. Right: $\nu = 100$, $meshsize = 25m$.

4 Multi-scale domain decomposition for embedded lagoons

In this section, we want to account for the possible multi-scale aspect of confinement. Indeed we considered here *Étang de Thau* as a lagoon of the Mediterranean Sea, but one could also focus on a small part of Thau and consider it as one of its sub-lagoons. On the other side, the Mediterranean Sea can be seen as a (large) lagoon of the North-Atlantic Ocean, etc.
There is thus a need to be able to compute a domain confinement while considering this multi-scale aspect. In the sequel, we will consider a reference lagoon Ω and perform a classical confinement computation (see above), providing C_Ω in Ω. Then, we will truncate the original domain in order to remove a small part ω of it, corresponding to a sub-lagoon, and compute the solution $C_{\Omega\setminus\omega}$ on the truncated domain $\Omega \setminus \omega$. If the new boundary conditions that are required on $\Omega \setminus \omega$ are well chosen, we will see that the two numerical solutions C_Ω and $C_{\Omega\setminus\omega}$ match in $\Omega \setminus \omega$.
The new boundary that is introduced when we remove ω from Ω has to be carefully studied. Indeed, we should implement absorbing boundary conditions (ABC) on it (see[EM77, HS89]). In practice, ABC are very difficult to find and implement; indeed, they lead to nonlocal boundary

operators (see [EM77]) that are not numerically suitable. But in our case, the velocity equation is very simple, and the corresponding ABC are no-slip boundary conditions:

$$\boldsymbol{u} \cdot n = \boldsymbol{u_n^{ext}}, \tag{6}$$

where $\boldsymbol{u_n^{ext}}$ is chosen accordingly with the volume of ω (the truncated part of the domain). These no-slip conditions for $\boldsymbol{u}$ write as non-homogeneous Neumann boundary conditions for the velocity potential (see [FR12]).
As far as the confinement field is concerned, we choose to impose an homogeneous Neumann condition on the new boundary. This is the simplest approximation of the ABC that one can use for advection-diffusion equations (see [Hal86]). We will consider improved boundary conditions (in the sense of [Hal86]), namely first order or second order conditions, in future works.

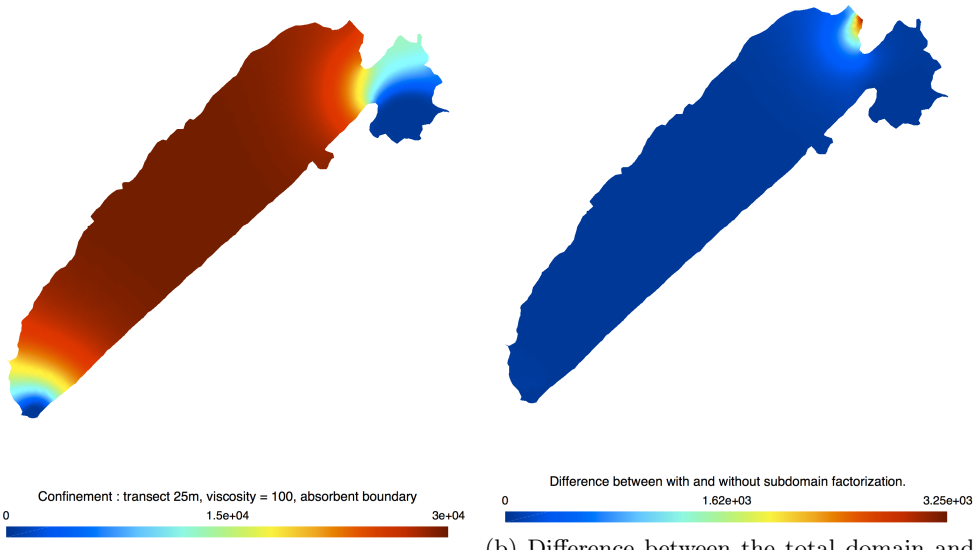

(a) Confinement

(b) Difference between the total domain and the factorization

Figure 5: Confinement in *Étang de Thau* with a fine mesh ($meshsize = 25m$), $\nu = 100$). Left: confinement computed in the truncated domain $\Omega \backslash \omega$ with homogeneous Neumann boundary conditions. Right: relative error between solutions computed in Ω and in $\Omega \setminus \omega$.

In Figure 5a we plot the confinement computed in the truncated domain $\Omega \backslash \omega$: it matches almost perfectly the previous simulations (see Figure 4d) in $\Omega \setminus \omega$. Actually, one can see in Figure 5b that there is a slight mismatch located by the new boundary ($\approx 10\%$ in L^∞ relative error, 0.6% in L^2 relative error), which is due to the approximation of the ABC (see discussion above).

Conclusion

We achieved two goals in this paper. On the one hand, we confirmed that the mathematical model introduced in [FR12] is suitable for the simulation of confinement in realistic lagoons such as *Étang de Thau*; the model may now be used and validated with realistic data (*i.e.* time series for the function θ, see Equation (3)). On the other hand, we introduced in Section 4 a method to perform multi-scale simulations of confinement in the case of embedded lagoons. We will consider theoretical and numerical improvements of this method (boundary conditions, use of homogenization methods) in future works.

Acknowledgments

The authors want to think the Languedoc-Roussillon region for providing data of *Étang de Thau*. They are also grateful to A. Fiandrino for very fruitful discussions related to this article.

References

[A.62] Jacques A. Hydrologie de l'étang de Thau. Revue des Travaux de l'Institut des Pêches Maritimes, 26, 1962.

[AAB+99] E. Abadie, Z Amzil, C Belin, M.-A. Comps, P. Elzière-Papayanni, P. Lassus, C. Le Bec, C. Marcaillou-Le-Baut, and E.and Poggi R. Nézan. Contamination de l'étang de Thau par Alexandrium tamarense. Technical report, Ifremer, 1999.

[Bar94] R. S. K. Barnes. A critical appraisal of the application of Guélorget and Pertuisot's concept of the paralic ecosystem and confinement to macrotidal europe. Estuarine, Coastal and Shelf Sciences, 38:41–48, 1994.

[DDG75] C. Delbos, A. Damasso, and J. Gilbert. Une ressouce alimentaire : la conchyliculture. CIHEAM - Options Mediterraneennes, 29:65–73, 1975.

[DPC93] J.-P. Debenay, J.-P. Perthuisot, and B. Colleuil. Expression numérique du confinement par les peuplements de foraminifères. app. aux domaines paral. actuels afri. w. C. R. Acad. Sci., Paris, série II, 316(2):1823–1830, 1993.

[EM77] B. Engquist and A. Majda. Absorbing boundary conditions for the numerical simulation of waves. Math. Comp., 31(139):629–651, 1977.

[FG07] E. Frénod and E. Goubert. A first step towards modelling confinement of paralic ecosystems. Ecological Modelling, 200(1-2):139–148, 2007.

[FR12] E. Frénod and A. Rousseau. Paralic confinement: Models and simulations. Acta Applicandae Mathematicae, pages 1–19, 2012. 10.1007/s10440-012-9706-2.

[GFP83] O. Guélorget, G. F. Frisoni, and J.-P. Perthuisot. La zonation biologique des milieux lagunaires : définition d'une échelle de confinement dans le domaine paralique méditérranéen. Journal de Recherche Océanographique, 8:15–36, 1983.

[GGLP90] O. Guélorget, D. Gaujous, M. Louis, and J.-P. Perthuisot. Macrobenthofauna of lagoons in guadaloupean mangroves (lesser antilles) : role and expression of confinement. Journal of Coastal Research, 6:611–626, 1990.

[GP83a] O. Guélorget and J.-P. Perthuisot. Le confinement, paramètre essentiel de la dynamique biologique du domaine paralique. Sciences Géologiques, Bulletin, 14:25–34, 1983.

[GP83b] O. Guélorget and J.-P. Perthuisot. Le domaine paralique. Expressions géologiques biologique, et économique du confinement. Presse de l'école normale supérieure 16-1983, 45 rue d'Ulm, Paris, 1983.

[Hal86] L. Halpern. Artificial boundary conditions for the linear advection diffusion equation. Math. Comp., 46(74):425–438, 1986.

[HPLH04] F. Hecht, O. Pironneau, and A. Le Hyaric. FreeFem++ manual. 2004.

[HS89] L. Halpern and M. Schatzman. Artificial boundary conditions for incompressible viscous flows. SIAM J. Math. Anal., 20(2):308–353, 1989.

[IGF+85] A. Ibrahim, O. Guélorget, G. G. Frisoni, J. M. Rouchy, A. Martin, and J.-P. Perthuisot. Expressions hydrochimiques, biologiques et sédimentologiques des gradients de confinement dans la lagune de guemsah (golfe de suez, egypte). Oceanologica Acta, 8:303–320., 1985.

[RD96] F. Redois and J.-P. Debenay. Influence du confinement sur la répartition des foraminifères benthiques : exemples de l'estran d'une ria mésotidale de Bretagne méridionale. Revue de Paléobiologie, 15(1):243–260, 1996.

[TSG09] D. Tagliapietra, M. Sigovini, and V. Ghirardini. A review of terms and definitions to categorise estuaries, lagoons and associated environments. Marine and Freshwater Research, 60(6):497–509, 2009.